*Int. J. Heat Mass Transfer.* Vol. 23, pp. 1195–1205
Pergamon Press Ltd. 1980. Printed in Great Britain

# TRANSIENT NATURAL CONVECTION HEAT TRANSFER IN A MASS OF WATER COOLED THROUGH 4°C

P. VASSEUR and L. ROBILLARD
Ecole Polytechnique, Université de Montréal, Department of Civil Engineering, Montreal, P.Q., Canada H3C 3A7

(*Received* 16 *October* 1979 *and in revised form* 23 *January* 1980)

**Abstract** — The transient two-dimensional laminar natural convection of water, enclosed in rectangular cavities with wall temperature maintained at 0°C is studied analytically. This investigation is carried out in order to study the inversion of flow patterns caused by the maximum density of water at 4°C. Numerical solutions are obtained for cases involving different aspect ratios and initial water temperatures varying between 4 and 21°C. Solutions of the governing coupled system of partial differential equations are obtained using an alternating direction implicit finite difference method. The results are presented graphically in the form of stream function and isotherm contour plots. The heat transfer through each wall is evaluated in order to study the effect of the density inversion on the cooling process. It is established numerically that one of the consequences of the nonlinearity of the water is to change the maximum heat transfer from the top wall of the cavity to the bottom one.

## NOMENCLATURE

$b$, enclosure width;
$B$, physical parameter, $g b^3/\alpha^2$;
$E$, aspect ratio of the half cavity;
$F_i$, body force;
$g$, acceleration due to gravity;
$Gr$, Grashof number, $\Delta\bar{\rho} g b^3/\nu^2$;
$k$, thermal conductivity at $\bar{T}$;
$l$, enclosure height;
$N_p$, number of horizontal grid spaces;
$M_p$, number of vertical grid spaces;
$p$, pressure;
$Pr$, Prandtl number;
$Ra$, Rayleigh number, $GrPr$;
$Ra'$, Rayleigh number, $RaPr$ modified;
$T$, temperature of fluid;
$\bar{T}$, mean temperature of fluid, $(T_i + T_w)/2$;
$T_i$, initial uniform water temperature;
$T_w$, temperature of enclosure;
$\Delta T$, temperature difference, $T_i - T_w$;
$t$, time;
$u_1, u_2$, velocities in $x_1$ and $x_2$ directions;
$U_1, U_2$, dimensionless velocities in $X_1$ and $X_2$ directions;
$x_1, x_2$, cartesian coordinates;
$X_1, X_2$, dimensionless cartesian coordinates.

Greek symbols

$\alpha$, thermal diffusivity;
$\beta$, volumetric coefficient of expansion of water;
$\mu$, dynamic viscosity at $\bar{T}$;
$\nu$, kinematic viscosity at $\bar{T}$;
$\bar{\rho}$, water density at $\bar{T}$;
$\rho$, density as a function of temperature;
$\Delta\bar{\rho}$, $(\bar{\rho} - \rho(\theta))/\bar{\rho}$;
$\tau$, dimensionless time;
$\phi_T, \phi_L, \phi_B$, dimensionless average heat transfer at the top, side and bottom wall respectively;
$\psi$, stream function;
$\bar{\Psi}$, dimensionless stream function;
$\omega$, vorticity;
$\Omega$, dimensionless vorticity;
$\theta$, dimensionless temperature;
$\theta_i$, dimensionless initial water temperature;
$\theta_w$, dimensionless temperature of enclosure.

Superscript

$^*$, refers to the pure conduction cases.

## INTRODUCTION

AN ENCLOSED, rectangular and fluid-filled cavity, through which heat is transferred by natural convection, is a simplified model of many practical situations and has been the subject of many theoretical investigations. The first formulation of this problem is due to Batchelor [1], although considerable attention had been, and is still being given to the analogous problem of the so-called Bénard cell [2], viz. convection in a fluid confined between two horizontal boundaries. Batchelor's attention was motivated by an interest in the thermal insulation which such cavities can provide. The first attempt to obtain a numerical solution of the relevant equations was made by Poots [3] from calculations performed on a desk-machine, but Wilkes [4] appears to have been the first to utilize an electronic computer. Since then the results of several other numerical investigations have been published (see for instance references [5–10]); that of Newel and Schmidt [11] contains a comprehensive bibliography.

In all those previous solutions a linear relationship between density and temperature has been assumed, such an assumption being acceptable for most fluids.

However, in the case of water near its freezing point a linear relationship is not justified. In fact, the density of water reaches a maximum value at 3.98°C, thereafter decreasing with decreasing temperature. It results from this nonlinearity that convective motion in water behaves in a rather peculiar manner when the temperature domain encompasses the 3.98°C point, for the density of water is a maximum at this temperature.

For recent literature on the effects of maximum density on free convection phenomenon, one may cite the works by Vanier and Tien [12, 13], Vasseur and Robillard [14] and Goren [15] who studied free convection about an isothermal vertical flat plate adjacent to a mass of cold water. Free convective heat transfer of a horizontal layer of maximum density liquid has been studied by Yen and Gorin [16], Adrian [17], Forbes and Cooper [18], Sugawara *et al.* [19] while Schenk and Schenkels [20], Yen and Galea [21] and Boger and Westwater [22] have published results concerning free convection induced by melting ice in cold water.

Concerning the effects of maximum density on convective motion of enclosed fluids, experimental work on the cooling of quiescent water in a pipe has been performed by Gilpin [23, 24] and Seki *et al.* [25] while a numerical solution to this problem has been presented by Cheng and Takeuchi [26]. The convective motion and heat transfer inside a rectangular cavity with vertical walls maintained at constant but different temperatures has been studied by Watson [27], Desai and Forbes [28] and Robillard and Vasseur [29]. In all these studies it was found that the effect of density inversion on the flow patterns, temperature profiles and average Nusselt number was unexpectedly large.

## FORMULATION OF THE PROBLEM

The problem to be considered is the motion and heat transfer which occurs when a mass of water, contained in a cavity, is cooled to near freezing. Initially the water is assumed to be at a uniform temperature $T_i$ and then the walls of the cavity are subjected to a constant temperature $T_w = 0°C$. Specifically, attention will be given to a rectangular cavity of depth $l$ and width $2b$, the aspect ratio of the half cavity being denoted by $E = l/b$.

It is supposed that the cavity is sufficiently long in the direction normal to the plane of the cavity for the motion to be assumed to be two-dimensional. It is also assumed that the motion is laminar. Experimental evidence (e.g. [30] and [31]) indicates that this assumption is valid provided the Rayleigh number based on cavity height is less than about $10^8$. In the following analysis it is assumed that $(T_i - T_w)$ is sufficiently small so that the Boussinesq approximation may be made, which neglects density variation in inertial terms of the equation of motion but retains it in the buoyancy term of the vertical equation. Water properties, with the exception of density in the buoyancy term, are assumed constant and are evaluated at the mean temperature $\bar{T} = (T_i + T_w)/2$. It is further assumed that all other relevant thermodynamic and transport properties are independent of temperature, and that compressibility and dissipation effects are negligible.

The equations expressing conservation of momentum, energy and mass are then:

$$\bar{\rho}\frac{Du_i}{Dt} = \rho(T)F_i - \frac{\partial p}{\partial x_i} + \mu\frac{\partial^2 u_i}{\partial x_j \partial x_j} \tag{1}$$

$$\frac{DT}{Dt} = \alpha\frac{\partial^2 T}{\partial x_j \partial x_j} \tag{2}$$

$$\frac{\partial u_i}{\partial x_i} = 0 \tag{3}$$

where $F_i = (-g, 0)$. The coordinates are so taken that $x_1$ is opposite to the direction of gravitational force.

Consistent with the previous assumptions, the density temperature relationship within the interested temperature range is assumed to be of the form:

$$\rho^{-1}(T) = \rho_0^{-1}\left[1 + \sum_{i=1}^{4}\beta_i T^i\right]. \tag{4}$$

The subscript '0' in (4) denotes a reference state (usually at 0°C).

The pressure $p$ is divided into two parts:

$$p = p' + p'' \tag{5}$$

where $p''$ is the deviation from original pressure $p'$.

Differentiating (5) with respect to $x_i$, substituting into (1) and taking the curl of the resulting equation, in order to eliminate the pressure term, yields for the two-dimensional motion under consideration:

$$\frac{D\omega}{Dt} = \frac{\partial}{\partial x_2}\left[\left(\frac{\bar{\rho} - \rho(T)}{\bar{\rho}}\right)g\right] + \nu\frac{\partial^2 \omega}{\partial x_j \partial x_j} \tag{6}$$

in which $\omega$ is the vorticity defined by:

$$\omega = -\frac{\partial^2 \psi}{\partial x_j \partial x_j} \tag{7}$$

where $\psi$ is the stream function such that:

$$u_1 = \frac{\partial \psi}{\partial x_2} \quad \text{and} \quad u_2 = -\frac{\partial \psi}{\partial x_1}. \tag{8}$$

It is noted that the equation of continuity is identically satisfied by the introduction of the stream function.

To make the governing equations dimensionless, the dimensionless time, velocities, distances, temperature, stream function and vorticity are defined as follows:

$$\tau = \frac{\alpha t}{b^2} \quad U_i = \frac{u_i b}{\alpha} \quad X_i = \frac{x_i}{b} \tag{9}$$

$$\theta = \frac{T - T_w}{T_i - T_w} \quad \bar{\Psi} = \frac{\psi}{\alpha} \quad \Omega = \frac{\omega b^2}{\alpha}$$

$$\Delta\bar{\rho} = (\bar{\rho} - \rho(\theta))/\bar{\rho} \qquad \nabla^2 = \frac{\partial^2(\ )}{\partial X_j \partial X_j}.$$

Substituting (9) into (2), (6) to (8) and making use of (4) gives:

Motion

$$\frac{D\Omega}{D\tau} = B\frac{\partial \Delta\bar{\rho}}{\partial X_2} + Pr\,\nabla^2\Omega. \tag{10}$$

Energy

$$\frac{D\theta}{D\tau} = \nabla^2\theta. \tag{11}$$

Vorticity

$$\Omega = -\nabla^2\bar{\Psi}. \tag{12}$$

Velocities

$$U_1 = \frac{\partial\bar{\Psi}}{\partial X_2}, \qquad U_2 = -\frac{\partial\bar{\Psi}}{\partial X_1}, \tag{13}$$

where $Pr = \nu/\alpha$ is the Prandtl number, and $B = (gb^3/\alpha^2)$, a physical parameter related to the size of the cavity.

The initial conditions are:

$$\tau = 0 \quad U_i = 0, \quad \bar{\Psi} = 0, \quad \Omega = 0, \quad \theta = 1 \quad \text{for} \quad 0 \leqslant X_1 \leqslant E, \quad 0 \leqslant X_2 \leqslant 1.0$$

and boundary conditions for $\tau > 0$

$$\begin{aligned}
&X_1 = 0 : \bar{\Psi} = 0, \quad U_1 = U_2 = 0 \quad \text{and} \quad \theta = \theta_w \\
&X_1 = E : \bar{\Psi} = 0, \quad U_1 = U_2 = 0 \quad \text{and} \quad \theta = \theta_w \\
&X_2 = 0 : \bar{\Psi} = 0, \quad U_2 = \Omega = 0 \quad \text{and} \quad \frac{\partial\theta}{\partial X_2} = 0 \\
&X_2 = 1.0 : \bar{\Psi} = 0, \quad U_1 = U_2 = 0 \quad \text{and} \quad \theta = \theta_w
\end{aligned} \tag{14}$$

in which use has been made of the symmetry of the problem with respect to a vertical plane passing through $X_2 = 0$. In view of the complex nature of the problem, a numerical solution appears to be the only approach for the present problem.

## NUMERICAL SOLUTION OF THE EQUATION

*Finite difference formulation*

In the present study a rectangular mesh system with spacing $\Delta X_1 = E/M_p$, $\Delta X_2 = 1/N_p$ is employed in the finite difference formulation of the governing equations and the appropriate boundary conditions. An implicit alternating direction (ADI) method is adopted for the finite difference solution of the parabolic type equations (10) and (11) and an iterative method [32] is used for the elliptic equation (12).

Boundary conditions on $\bar{\Psi}$ and $\theta$ are applied in the usual manner, using central differences, when it is possible, and image points for derivative conditions. Vorticity boundary conditions were first obtained using the method introduced by Gosman *et al.* [33]. The results obtained with this approximation were excellent for fluids having a linear relationship between density and temperature. However for the case of convection with an inversion density effect it was observed that the vorticity equation exhibited a boundary induced instability at relative low $\Delta\tau$. The same situation has been encountered in the past by Samuel in his study on the stability of a layer of fluid heated from below [34]. As shown by this author this type of problem may be solved by using a lower order approximation for the vorticity on the boundary.

In order to check the validity of the present numerical method, comparisons have been made with other existing solutions. For low Rayleigh numbers ($\sim 10^4$), an excellent agreement was observed with the analytical Poots' solution [3] for a square cavity. For higher Rayleigh numbers, ($\sim 10^6$), the numerical results from Wilkes [4], for the case of heat transfer into a rectangular cavity, were integrally reproduced.

*Effect of mesh size*

The determination of an acceptable mesh size is of prime importance since the greater computational accuracy obtainable with larger values of $N$ and $M$ must be balanced against computer time. The calculations were carried out using a $20 \times 20$ mesh; i.e. the cell size was $b/20$ and $l/20$. Rubel and Landis [8] showed that the use of a finer mesh made relatively little difference to the final results. It was found by Wilkes [4] that the use of a $10 \times 10$ grid gives results remarkably close to that of a $20 \times 20$ grid, a 15% difference in the heat transfer at walls between the two being however observed.

*Density–temperature relationship*

The temperature dependent density for water in equation (4) can be approximated by the following equation for the temperature range $0 \sim 20°C$:

$$\rho^{-1} = \rho_0^{-1}(1 + \beta_1 T + \beta_2 T^2 + \beta_3 T^3 + \beta_4 T^4) \tag{15}$$

where: $\rho_0 = 0.9998396$ (g cm$^{-3}$);
$\beta_1 = -0.678964520 \times 10^{-4}$ (1/°C);
$\beta_2 = 0.907294338 \times 10^{-5}$ (1/°C$^2$);
$\beta_3 = -0.964568125 \times 10^{-7}$ (1/°C$^3$) and
$\beta_4 = 0.873702983 \times 10^{-9}$ (1/°C$^4$).

Fujii [35] notes that the foregoing expression agrees with the tabulated data of Landolt-Börnstein [36] with an error of less than one unit at the last digit.

## RESULTS AND DISCUSSION

The results are more meaningful if presented in the form of transient streamlines and isotherms. Streamlines are important as they give an immediate picture of the flow pattern in the enclosure. Isotherms are also important as they indicate the density distribution

Table 1. Physical parameters

| Case | $T_i$ | $T_w$ | $gb^3/\alpha^2$ | $E$ |
|---|---|---|---|---|
| 1 | 10° | 0° | $5.32 \times 10^8$ | 2 |
| 2 | 10° | 0° | $5.32 \times 10^8$ | 6 |
| 3 | 4° | 0° | $1.80 \times 10^9$ | 2 |
| 4 | 10° | 0° | $1.80 \times 10^9$ | 2 |
| 5 | 8° | 0° | $1.80 \times 10^9$ | 2 |
| 6 | 10° | 0° | $6.65 \times 10^7$ | 2 |
| 7 | 10° | 0° | $5.32 \times 10^8$ | 4 |
| 8 | 21° | 20° | $4.79 \times 10^8$ | 2 |

inside the flow field. Specifically, the 4°C isotherm, when superposed to the streamline pattern, will give the location of the maximum density. This particular isotherm, when it exists, is shown as a heavy dashed line on the plots of the streamlines as well as on the isotherm plots.

To expedite plotting of the results, an auxiliary computer program was written to locate points lying on specified isotherms and streamlines. As mentioned earlier the problem under consideration is symmetrical and it was found advantageous to reproduce computer results at a given time on a single graph with the flow pattern on the right half of the cavity and the isotherms on the left half.

Consideration will be given first to case 1 of Table 1 which corresponds to a square cavity ($E = 2$) with initial water temperature $T_i = 10$°C and wall temperature maintained continuously at $T_w = 0$°C, this case providing rather typical and interesting results. The Prandtl number $Pr$ is taken to be 11.6, corresponding to the average temperature 5°C. The computed results for the mean temperature $\theta_M$, the center point temperature $\theta_C$, the maximum temperature $\theta_{max}$, the heat transfer $\phi_T$, $\phi_B$ and $\phi_L$ related to the top, lower and lateral boundaries respectively are shown in Fig. 1 as functions of the dimensionless time $\tau$. The corresponding curves for pure conduction have been also included in this graph for comparison purpose. In the case of pure conduction the heat transfer is the same for all the boundaries and is denoted by $\phi^*$, all other variables with the superscript (*) also referring to the pure conduction. It is noted that the mean temperature $\theta_M$ is proportional to the heat in excess of $\theta_w$, remaining in the cavity at time $\tau$. Its slope is directly related to the heat transfer at the boundaries by the following expression:

$$E\frac{\partial\theta_M}{\partial\tau} = -[E\phi_L + \phi_T + \theta_B]. \tag{16}$$

The difference between the pure conduction curve $\theta_M^*$ and the actual $\theta_M$ curve is proportional to the additional heat transfer through the boundaries, attributed exclusively to convection that has occurred from the initiation of the cooling process to the time considered. It is seen that, due to the fluid circulation inside the cavity, the upper and lower boundary heat transfers $\phi_T$ and $\phi_B$ take values quite different from that of the pure conduction heat transfer $\phi^*$. It is also noticed that the heat transfer $\phi_L$ on the vertical wall is less affected by convection and consequently follows

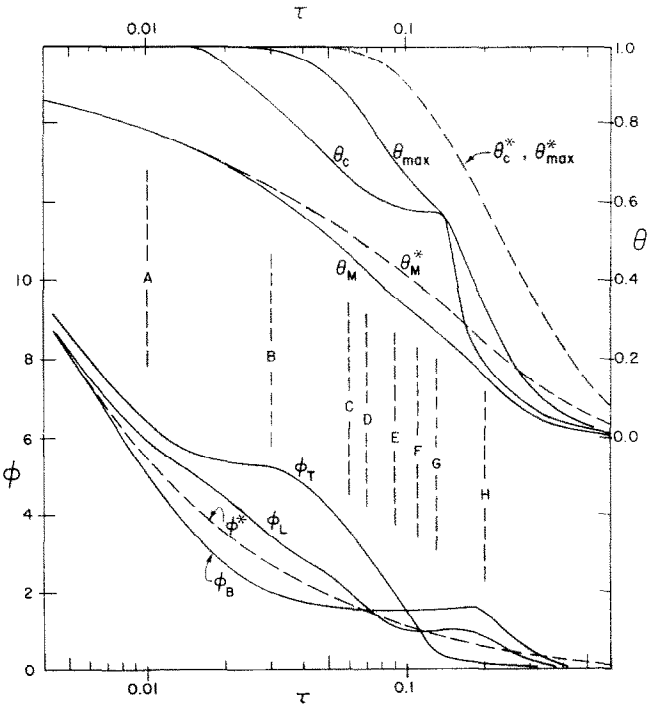


FIG. 1. Transient distributions for $\theta_C$, $\theta_M$, $\theta_{max}$, $\phi_T$, $\phi_L$ and $\phi_B$ with results from pure conduction for case 1.

more closely the pure conduction heat transfer curve and stays approximately at a mean value between $\phi_T$ and $\phi_B$.

Typical sets of the resulting streamlines and isotherms corresponding to different times $\tau$ are shown in Fig. 2. The maximum and minimum values of the stream function and the contour intervals $\Delta\bar{\Psi}$ for each graph are given in Table 2. It should be noted that for this type of problem, the boundaries of the cavity always correspond to the $T_w$ isotherm. Figure 3 gives (a) the velocity profiles $U_1$ along the horizontal centerline passing through $X_1 = 0.5$, (b) the velocity profiles $U_2$ along a vertical centerline located at the position $X_2 = 0.5$ and (c) the transient temperature profiles along the horizontal centerline already mentioned. The symbols A, B, C, etc. shown in Figs. 1 and 3 correspond to the sequence of the transient streamline patterns and isotherms of Fig. 2. Those figures may thus be contrasted with each other to gain some insight into the flow and temperature fields.

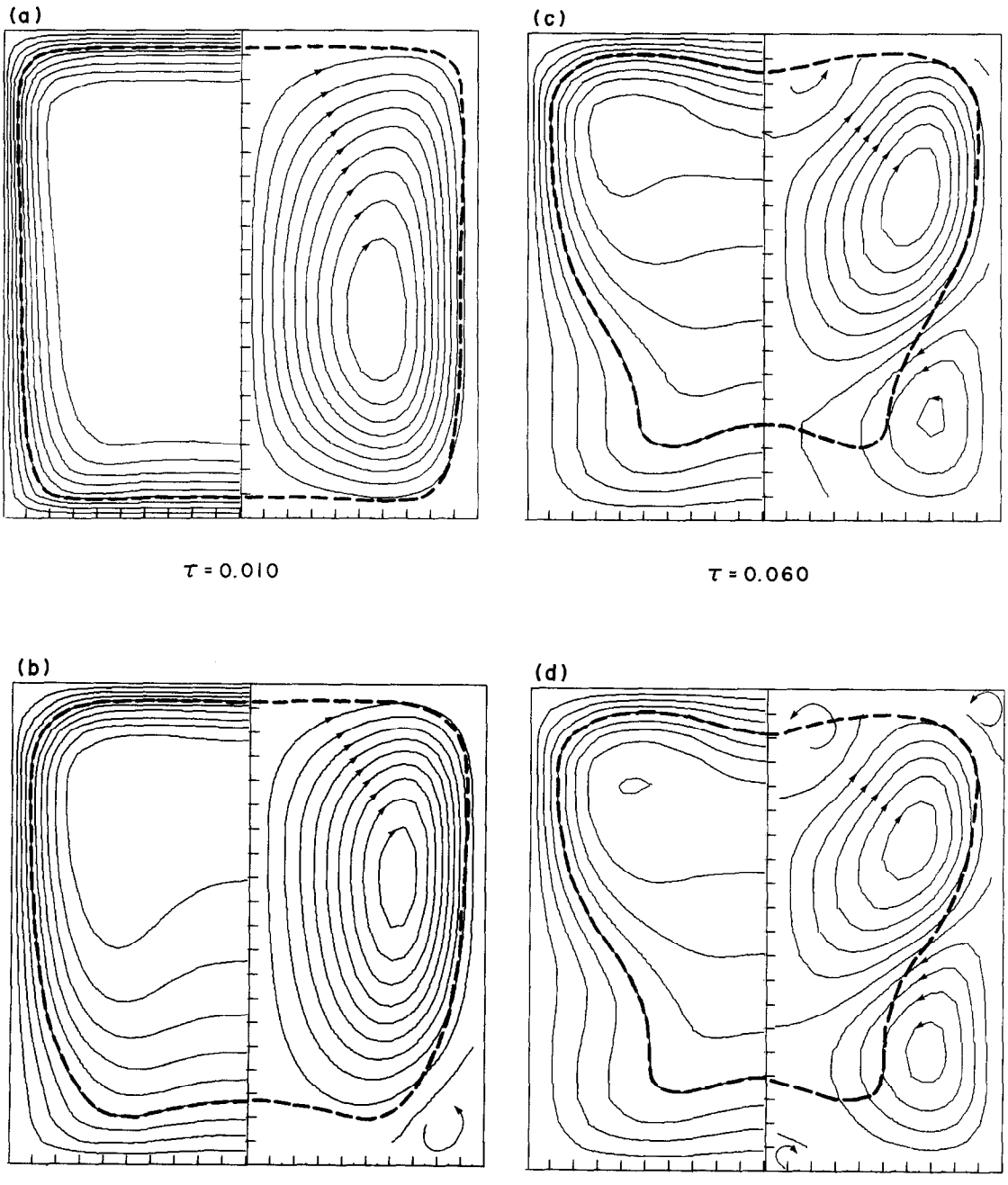


FIG. 2(a–d).

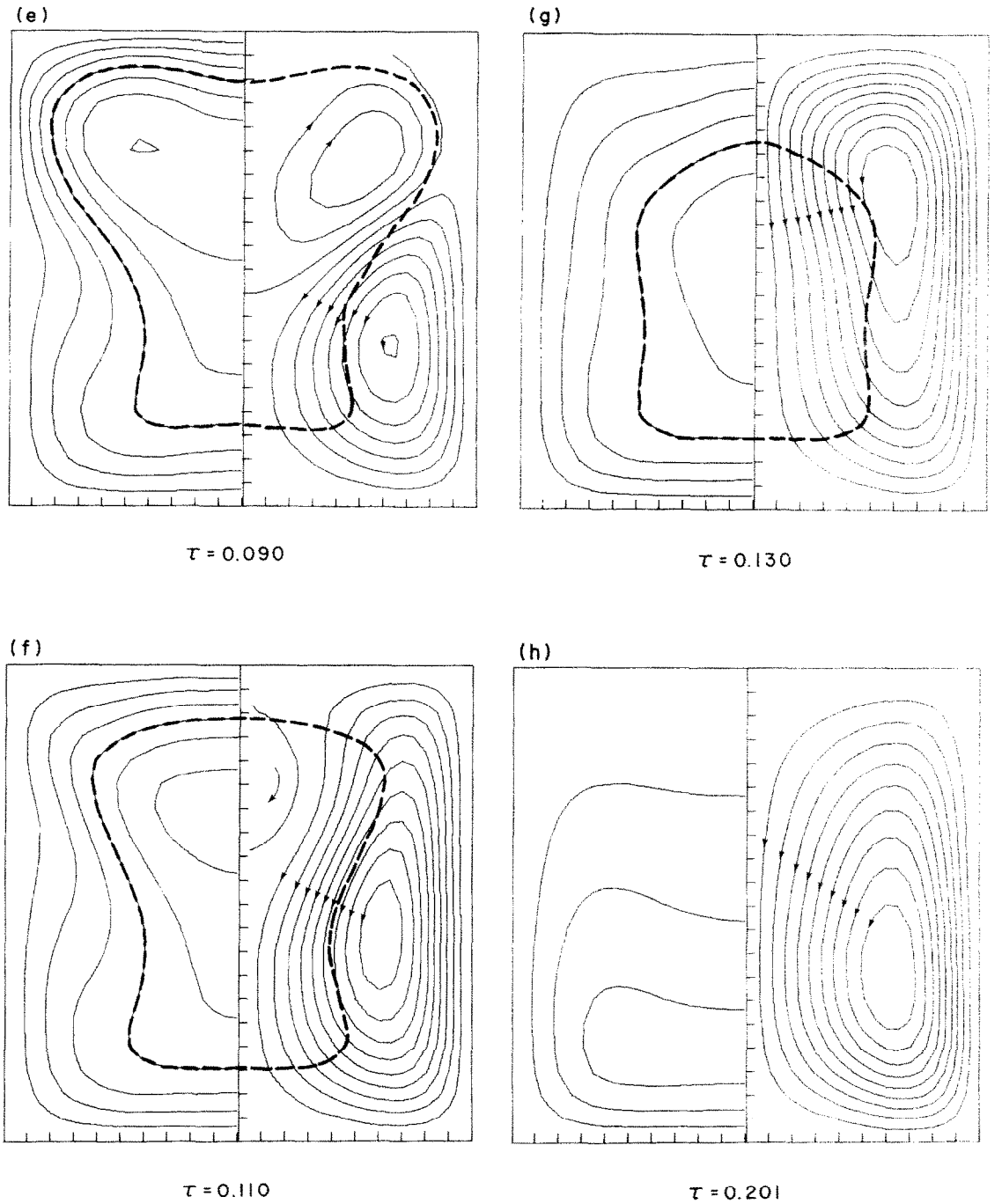


FIG. 2(e–h).

FIG. 2. Transient streamline pattern and isotherms for case 1.

At the very beginning of the cooling process, heat transfer is dominated by conduction. A motion of the boundary layer type is first set up near the walls, this movement gradually extending inside the cavity. At the end of what might be called an initial regime, that is, approximately at point A in Figs. 1 and 3 ($\tau \simeq 0.01$), motion has become important over the entire cavity. Two counter rotating vortices are then present in the whole enclosure, as it can be deduced from Fig. 2a which only shows the right clockwise vortex. It is seen on Fig. 3c that the temperature profile A still reveals thermal boundary layer characteristics whereas the velocity profile (curve A of Fig. 3a) shows an important gradient near the side boundary, this gradient being a remnant of the initial boundary layer already mentioned. It results from the motion shown on Fig. 2a that the cooler water is transported downward while the warmer water in the core region is transported

Table 2. Maximum and minimum values of stream functions and maximum dimensionless temperatures for cases 1 and 2

| Fig. No. | $\tau$ | $\bar{\Psi}_{max}$ | $\bar{\Psi}_{min}$ | $\Delta\bar{\Psi}$ | $\theta_{max}$ |
|---|---|---|---|---|---|
| 2a | 0.01 | 27.00 | − 0.02 | 2.70 | 1.00 |
| 2b | 0.03 | 21.00 | − 0.90 | 3.00 | 0.99 |
| 2c | 0.06 | 8.90 | − 9.20 | 1.80 | 0.86 |
| 2d | 0.07 | 6.90 | − 5.40 | 1.20 | 0.80 |
| 2e | 0.09 | 3.00 | − 7.40 | 1.04 | 0.70 |
| 2f | 0.11 | 0.25 | − 8.40 | 0.86 | 0.64 |
| 2g | 0.13 | 0.00 | − 9.20 | 0.92 | 0.59 |
| 2h | 0.20 | 0.00 | − 6.40 | 0.64 | 0.35 |
| 4a | 0.05 | 37.00 | − 8.50 | 4.50 | 0.99 |
| 4b | 0.10 | 18.00 | − 17.00 | 3.50 | 0.87 |
| 4c | 0.15 | 9.00 | − 21.00 | 3.00 | 0.73 |
| 4d | 0.30 | 0.00 | − 13.00 | 1.30 | 0.40 |

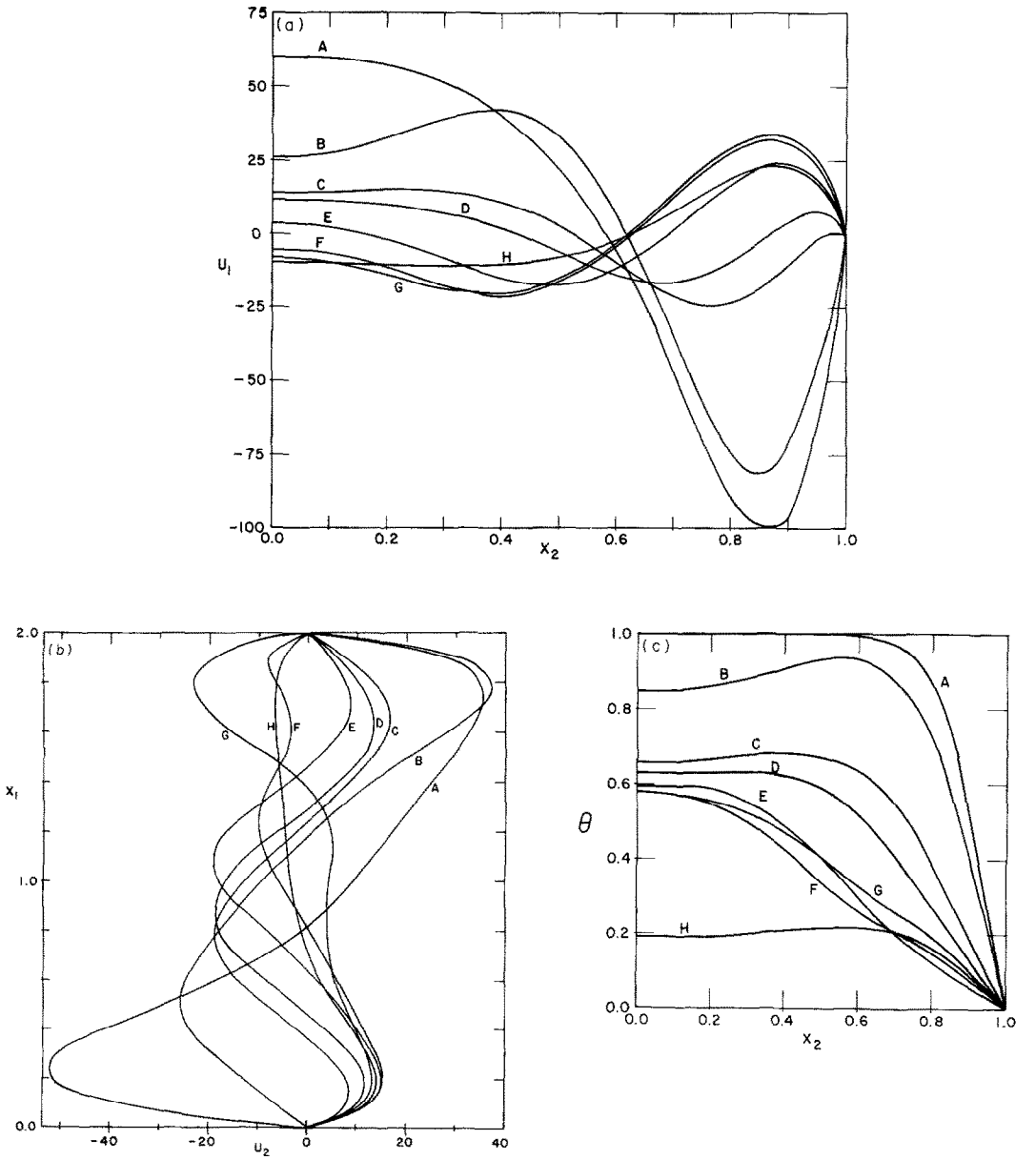


FIG. 3. Transient velocity profiles (a, b) and temperature profiles (c) for case 1.

upward. Thus, as shown in Fig. 2b a large part of the body of water has become thermally stratified with the isotherms sparsely spaced near the bottom wall and closely spaced near the top one. This configuration indicates qualitatively that the local heat transfer is higher at the top wall than at the bottom one. Quantitatively the values of these local wall heat fluxes are given on Fig. 1 by the curves $\phi_T$, $\phi_B$ and $\phi_L$ at location B. At this stage of the cooling process it is of interest to go back to the isotherm field shown in the left half on Fig. 2a. It is noted that at the bottom of the cavity, in the layer of fluid included between the 4°C isotherm and the 0°C bottom boundary, the buoyancy force changes sign and the flow field is potentially unstable because of the top-heavy situation similar to the well-known case with heating from below [34]. Thus, the intensity of flow near the bottom remains rather weak until the vertical density gradient becomes sufficiently large. This unstable layer then grows and an additional pair of vortices rotating opposite to the existing earlier one appears, marking the beginning of the inversion process. The resulting flow pattern is depicted on Fig. 2b.

With the progression of the cooling process, the lower vortex appearing on the right half of Fig. 2b gradually increases its intensity and displaces the upper vortex (see sketches c, d, e and f of Fig. 2). The cooler water located near the vertical wall and between the two counter rotating vortices is carried directly into the core region and disturbs locally the flow field as it can be observed by the distortion of the isotherms (see for instance curve E, Fig. 3c). Furthermore, due to the combined action of the counter-rotating vortices, some of the warmer core water is carried downward in the lower portion of the cavity. It results from this motion that the heat transfer rate at the lower wall $\phi_B$ improves subsequently as shown in Fig. 1. At the time step $\tau \approx 0.1$, the curves $\phi_T$ and $\phi_B$ cross each other and the heat transfer rate $\phi_B$ on the lower wall becomes greater than $\phi_T$ and $\phi_L$.

At $\tau = 0.110$ Fig. 2f shows that the original clockwise vortex has almost completely been engulfed by the already strong vortex grown from below. The original clockwise circulation is completely reversed in Fig. 2g indicating that the flow field inversion process has come to an end. In Fig. 2h it is seen that the relatively warm core has moved in the lower region and that the stratification of the water is now characterized by weak gradients at the top of the cavity and strong gradients at the bottom. Thus the temperature field also shows characteristics opposite to its earlier stages (see Fig. 2b). It is of interest to note that the vortex motion at the beginning (Fig. 2a) and at the end of the cooling process (Fig. 2h) although opposite in direction are similar in character (see also Fig. 3a and b). Results obtained for higher values of $\tau$ (not presented here) show that the momentum of the eddy motion is slowly dissipated by the opposing viscous forces and that the fluid motion becomes more and more minute.

In addition to the two most significant vortices already discussed, some other eddies of very small intensity are also present in the corners of the half cavity (see Fig. 2d). It is true that the existence of artificial corner cells, caused by numerical computation, has been reported in the past in literature [8]. However, the size of the grid mesh used in the present computation has been chosen in order to avoid this problem.

The effect of the cavity size $b$ on the flow pattern and the heat transfer has been studied numerically (cases 1, 4 and 6 of Table 1). The numerical values obtained are not reported graphically here but the general trend of these results will be discussed. It was found that for fixed values of $T_w$ and $T_i$ an increase of the physical parameter $gb^3/\alpha^2$ (which corresponds to an increase of the cavity size $b$) strengthens the convection of the flow, and consequently the overall heat transfer, at the early stages of the cooling process. Thus with $b$ increasing, the heat transfer curves $\phi_T$ and $\phi_B$ move away from the pure conduction heat transfer curve $\phi^*$. It is also observed that when $gb^3/\alpha^2$ is increased, the difference $(\theta_M^* - \theta_M)$ becomes more important. Furthermore it is observed that the crossing of the two curves $\phi_T$ and $\phi_B$, which is a consequence of the inversion of the circulation inside the cavity, occurs earlier. For the largest value $gb^3/\alpha^2$ used in the computation (case 4), the curve $\phi_T$ is characterized by a sudden increase that occurs shortly after the initiation of the cooling process and that lasts for a relatively short period of time. This bump of the curve $\phi_T$ has the tendency to develop into a sharp peak when the value of $gb^3/\alpha^2$ is further increased. Such behavior may be explained in the following way. At the very beginning of the cooling process, only conduction is present and the curves $\phi_B$, $\phi_T$ and $\phi_L$ originate from the same values. When fluid motion develops, those curves separate one from the other, heat being transported toward the top boundary through the action of gravity forces. If fluid motion is strong enough, warmer fluid may take the place of cooler fluid in the vicinity of the top boundary. For such situations this means that the cooling by conduction becomes a slower process than the supply of heat by convection. In those conditions the heat transfer may increase drastically through a given boundary. A similar effect has been observed for the lower boundary heat transfer $\phi_B$ when the temperature range is between 4 and 0°C.

The influence of the aspect ratio $E$ on the present problem has been studied in cavities with $E = 4$ and $E = 6$ (cases 2 and 7, of Table 1). Figure 4 presents the flow patterns and isotherms for the case $E = 6$. It is noticed that the general features remain similar to those of the square cavity ($E = 2$). However it was observed from numerical results, not presented here, that when $E$ is increased the inversion process requires a longer period of time to be accomplished. The growing and the spreading of the counter clockwise vortex in the entire cavity appears to be a slower process than in the case of a square cavity.

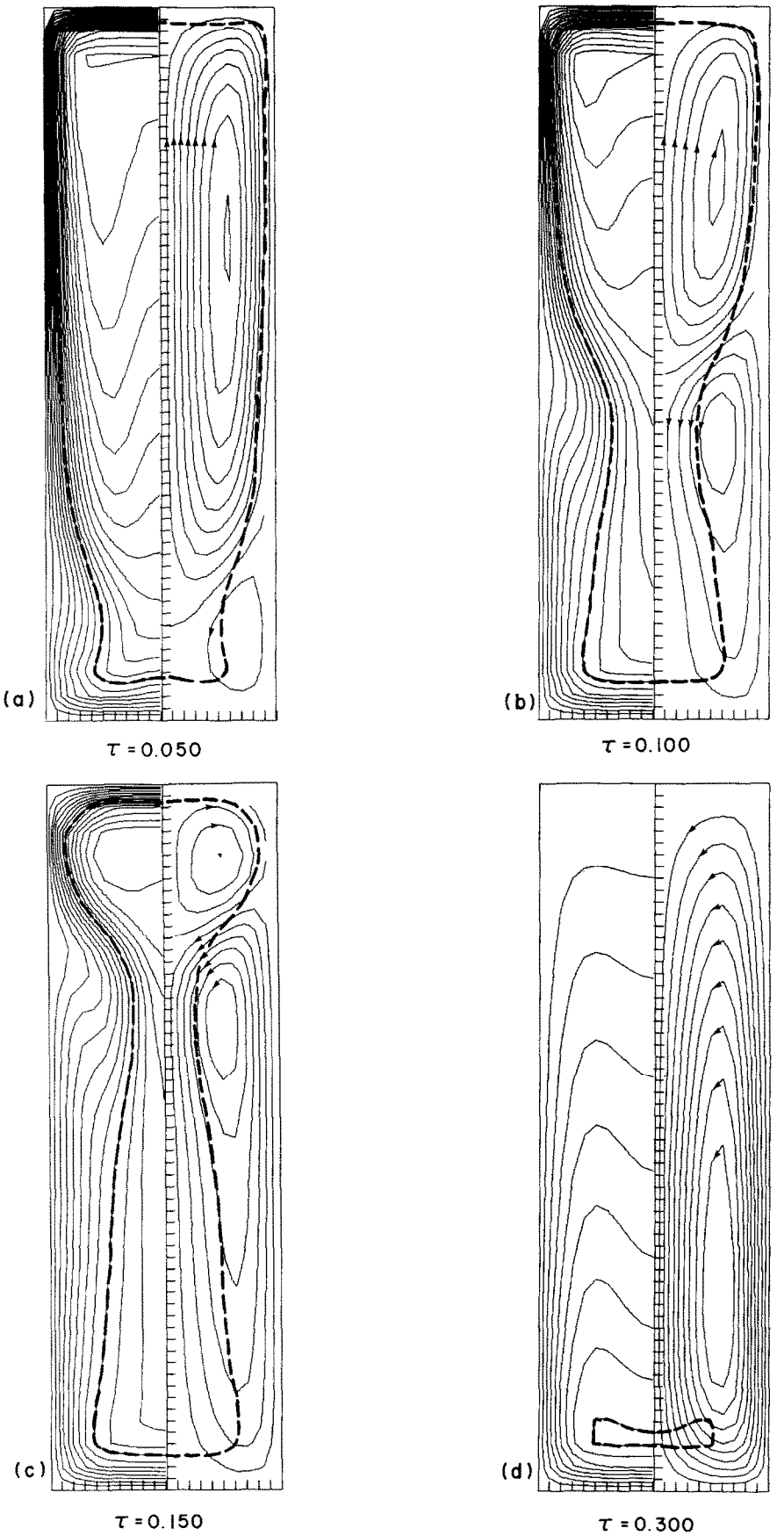


FIG. 4. Transient streamline pattern and isotherms for case 2.

## CONCLUSIONS

The results obtained in the present study can be summarized as follows:

1. Convective heat transfer is greatly influenced by the presence of density maximum in the convective fluid.

2. When the temperature corresponding to the maximum density is between $T_i$ and $T_w$, the flow pattern and temperature field which start in a way comparable to linear free convection tend to a final state which corresponds to a completely reversed situation in all aspects.

3. By comparison to equivalent situations in the linear range of temperature, it can be deduced that the change in rotation affecting the convective cells retards the cooling process of the cavity.

*Acknowledgement* — This research was supported by the National Research Council of Canada through grants NRC A-9201 and NRC A-4197.

## REFERENCES

1. G. K. Batchelor, Heat transfer by free convection across a closed cavity between vertical boundaries at different temperatures, *Q. Appl. Math.* **12,** 209–233 (1954).
2. H. Bénard, Les tourbillons cellulaires dans une nappe liquide, *Rev. Gén. Sci.* **11,** 1261 (1900).
3. G. Poots, Heat transfer by laminar free convection in enclosed plane gas layer, *Q. Jl Mech. Appl. Math.* **11,** 257–273 (1958).
4. J. D. Wilkes, The finite difference computations of natural convection in an enclosed rectangular cavity, Ph.D. Thesis, University of Michigan (1963).
5. R. W. Thomas and G. DeVahl Davis, Natural convection in annular and rectangular cavities, a numerical study, *Heat Transfer*, 4, paper NC2.4, pp. 1–11, Elsevier, Amsterdam (1970).
6. G. D. Mallison and G. De Vahl Davis, The method of the false transient for the solution of coupled elliptic equations, *J. Comp. Phys.* **12,** 435–461 (1973).
7. G. De Vahl Davis, Laminar natural convection in an enclosed rectangular cavity, *Int. J. Heat Mass Transfer* **11,** 1675–1693 (1968).
8. A. Rubel and F. Landis, Numerical study of natural convection in a vertical rectangular enclosure, *High Speed Comp. Fluid Dynam.* **II,** 208–213 (1969).
9. D. Greenspan, Numerical studies of prototype cavity flow problems, *Comp. Sci. J.* **92,** 88–93 (1968).
10. K. Aziz and J. D. Hellums, Numerical solution of the three-dimensional equations of motion for laminar natural convection, *Physics Fluids* **10**(2), 314–324 (1967).
11. M. E. Newel and J. Schmidt, Heat transfer by laminar natural convection within rectangular enclosures, *J. Heat Transfer* **92,** 159–168 (1970).
12. C. R. Vanier and C. Tien, Effects of maximum density and melting on natural convection heat transfer from a vertical plate, *Chem. Engng Prog. Symp. Ser.* No. 82, 64 (1968).
13. C. R. Vanier and C. Tien, Further work on free convection in water at 4°C, *Chem. Engng Sci.* **22,** 1747–1751 (1967).
14. P. Vasseur and L. Robillard, Natural convection of water near the freezing point, *IAHR Symp. Ice Problems*, Lucla, Sweden, 257–270 (1978).
15. S. L. Goren, On free convection in water at 4°C, *Chem. Engng Sci.* **21,** 515–518 (1966).
16. Y. C. Yen and F. Gorin, Onset of convection in a water layer formed continuously by melting, *Physics Fluids* **12,** 509–516 (1969).
17. R. J. Adrian, Turbulent convection in water over ice, *J. Fluid Mech.* **69,** 753–781 (1975).
18. R. E. Forbes and J. W. Cooper, Natural convection in a horizontal layer of water cooled from above to near freezing, *J. Heat Transfer* **97,** 47–53 (1975).
19. M. Sugawara, S. Fukusako and N. Seki, Experimental studies on the melting of a horizontal ice layer, *Bull. J.S.M.E.* **18**(121), 714–721 (1975).
20. C. Schenk and A. Schenkels, The effect of maximum density on natural convection, *Chem. Engng Prog. Symp. Ser.* No. 117, 84 (1968).
21. Y. C. Yen and F. Galea, Onset of convection in a water layer formed continuously by melting ice, *Physics Fluids* **12,** 509–516 (1969).
22. D. V. Boger and J. W. Westwater, Effect of buoyancy on the melting and freezing process, *J. Heat Transfer* **89,** 81–89 (1967).
23. R. R. Gilpin, Cooling of a horizontal cylinder of water through its maximum density point at 4°C, *Int. J. Heat Mass Transfer* **18,** 1307–1315 (1975).
24. R. R. Gilpin, The effects of dentritic ice formation in water pipes, *Int. J. Heat Mass Transfer* **20,** 693–699 (1977).
25. N. Seki, S. Fukusako and M. Nakaoka, Experimental study on natural convection heat transfer with density inversion between two horizontal cylinders, *J. Heat Transfer* **97,** 556–561 (1975).
26. K. C. Cheng and M. Takeuchi, Transient natural convection of water in a horizontal pipe with constant cooling rate through 4°C, *J. Heat Transfer* **98,** 581–587 (1976).
27. A. Watson, The effect of the inversion temperature on the convection of water in an enclosed rectangular cavity, *Q. Jl Mech. Appl. Math.* **25,** 523–446 (1972).
28. V. S. Desai and R. E. Forbes, Free convection in water in the vicinity of maximum density. Environmental and geophysical heat transfer, *Trans. Am. Soc. Mech. Engrs* 41–47 (1971).
29. L. Robillard and P. Vasseur, Effet du maximum de densité sur la convection libre de l'eau dans une cavité fermée, *Can. J. Civil Engng.* **6**(4), 481–493 (1979).
30. J. W. Elder, Laminar free convection in a vertical slot, *J. Fluid Mech.* **23,** 77–98 (1965).
31. F. Landis and H. Lanowitz, Transient natural convection in a narrow vertical cell, *Proc. 3rd Int. Heat Transf. Conference*, A.I.Ch.E., New York (1966).
32. B. Carnahan, H. A. Luther and J. O. Wilkes, *Applied Numerical Methods*, John Wiley, New York (1969).
33. A. D. Gosman, W. M. Pun, A. K. Runchal, D. B. Spalding and M. Worfshtein, *Heat and Mass Transfer in Recirculating Flows*, Academic Press, London (1969).
34. M. R. Samuels and S. W. Churchill, Stability of a fluid in a rectangular region heated from below, *A.I.Ch.E. Jl* **13,** 77–85 (1967).
35. T. Fujii, Fundamentals of free convection heat transfer, *Prog. Heat Transfer Engng* **3,** 66–67 (1974).
36. Landolt-Börnstein, *Zahlenwerte und Funktionen*, Vol. II, pp. 36–37, Springer, Berlin (1971).

## CONVECTION THERMIQUE NATURELLE VARIABLE DANS UNE MASSE D'EAU REFROIDIE AUTOUR DE 4°C

**Résumé**—On étudie théoriquement la convection naturelle laminaire, bidimensionnelle, variable pour l'eau confinée dans une cavité rectangulaire, avec une paroi maintenue à 0°C. Cette étude est menée de façon à étudier l'inversion des configurations d'écoulement causée par le maximum de densité à 4°C. Des solutions numériques sont obtenues pour différents rapports d'allongement et différentes températures initiales d'eau entre 4°C et 21°C.

Les solutions des équations aux dérivées partielles sont obtenues en utilisant la méthode implicite aux différences finies avec direction alternée. Les résultats sont présentés graphiquement sous la forme de lignes de courant et de lignes isothermes. Le transfert thermique est évalué sur chaque paroi pour étudier l'influence de l'inversion sur le processus de transfert. Il est établi numériquement que l'effet est de changer le transfert maximal de la paroi supérieure de la cavité, vers la paroi inférieure.

## WÄRMEÜBERTRAGUNG DURCH FREIE KONVEKTION IN EINER UNTER 4°C ABGEKÜHLTEN WASSERMASSE

**Zusammenfassung**—Die instationäre, zweidimensionale, laminare freie Konvektion von Wasser, das in rechteckigen Hohlräumen mit auf 0°C gehaltenen Wandtemperaturen eingeschlossen ist, wird analytisch untersucht. Diese Arbeit wird durchgeführt, um die Inversion der Strömungsverläufe, die vom Dichtemaximum des Wassers bei 4°C herrührt, zu untersuchen. Es werden numerische Lösungen für Fälle, die verschiedene Seitenverhältnisse und zwischen 4°C und 21°C variierende Wasseranfangstemperaturen umfassen, erhalten. Die Lösungen des beschreibenden gekoppelten Systems von partiellen Differentialgleichungen werden erhalten, indem eine richtungs-alternierende, implizite, endliche Differenzenmethode benutzt wird. Die Ergebnisse sind grafisch in Stromfunktions- und Isothermen-Kurvenscharen dargestellt. Die Wärmeübertragung durch jede Wand wird bestimmt, um den Einfluß der Dichteinversion auf den Abkühlvorgang zu untersuchen. Es wird numerisch untermauert, daß eine der Konsequenzen der Nichtlinearität von Wasser die ist, daß sich das Maximum der Wärmeübertragung von der oberen Behälterwand zu der unteren verlagert.

## ТЕПЛОПЕРЕНОС ПРИ НЕСТАЦИОНАРНОЙ ЕСТЕСТВЕННОЙ КОНВЕКЦИИ В ОБЪЕМЕ ВОДЫ, ОХЛАЖДЕННОЙ НИЖЕ 4°С

**Аннотация** — Аналитически исследовалась нестационарная двумерная ламинарная естественная конвекция в объемах воды, помещенных в прямоугольные замкнутые полости с температурой стенок, равной 0°С. Целью исследования являлось изучение структур течения, вызванных максимальной плотностью воды при 4°С. Получены численные решения для различных отношений сторон полостей и начальных температур воды в диапазоне от 4°С до 21°С.

С помощью конечно-разностного неявного метода переменных направлений получены решения системы дифференциальных уравнений в частных производных. Результаты представлены в графическом виде. Дана оценка величины теплового потока через каждую стенку с целью определения влияния инверсии плотности на процесс охлаждения. В результате численных расчетов установлено, что из-за нелинейности воды происходит смещение максимума теплообмена с верхней стенки полости к нижней.